

# Simple Fabrication of Molecular Circuits by Shadow Mask Evaporation

Y. X. Zhou<sup>†</sup> and Alan T. Johnson, Jr.\*

*Department of Physics and Astronomy and Laboratory for Research on the Structure of Matter, University of Pennsylvania, Philadelphia, Pennsylvania 19104*

**James Hone**

*Department of Mechanical Engineering, Columbia University, New York, New York 10027*

**Walter F. Smith**

*Department of Physics, Haverford College, Haverford, Pennsylvania 19041*

*Received July 14, 2003; Revised Manuscript Received August 7, 2003*

## ABSTRACT

We fabricate contacts to molecular circuits by evaporating metal through a nanoscale stencil mask etched in a free-standing silicon nitride membrane. In this way, contacts can be fabricated on as-grown molecular wires that would be contaminated or destroyed by chemicals and heat treatments associated with conventional lithographic techniques. Chemical vapor deposition-grown single-walled carbon nanotubes contacted in this fashion behave similarly to samples contacted using conventional lithography but are more robust to failure at high bias. In-vacuum electrical measurements of  $\lambda$ -DNA networks on mica substrates contacted in a “leads-on-top” geometry give a lower bound of 1000 T $\Omega$  for the resistance of a 1- $\mu$ m length of DNA.

Molecular devices are frequently based on nanowires or nanotubes that are grown or deposited on a substrate and subsequently contacted using electron-beam or optical lithography. In these approaches, a polymer resist layer is applied to the sample and then baked; after exposure, the resist is developed using organic solvents. This can potentially alter the nanowire under investigation or even destroy particularly delicate samples. It would be advantageous to deposit nanoscale metal contacts directly without the damage associated with the chemistry and thermal stresses of conventional lithography.

Here we describe a process to accomplish this goal based on metal evaporation through a free-standing nanoscale stencil created in a suspended silicon nitride membrane. Other groups have demonstrated the ability to create such shadow masks with features as small as 20 nm and have used them to fabricate metal nanostructures and wires.<sup>1–4</sup> In this work, we take advantage of the fact that nanowires contacted in this way are exposed only to the ambient atmosphere and the evaporated metal. We use stencil masks to fabricate nanoscale contacts to pristine single-walled carbon nanotubes (SWNTs) grown by chemical vapor

deposition (CVD) as well as delicate networks of  $\lambda$ -DNA in a “leads-on-top” geometry. Nanotube samples contacted by shadow mask evaporation behave similarly to those contacted by conventional means, although they appear to be significantly more robust against failure under high bias. We find that  $\lambda$ -DNA samples conduct very poorly, and we argue that the measured conduction in air is predominantly due to water adsorbed on the hydrophilic molecule and mica substrate. We measure a small residual conductivity under vacuum that may be intrinsic to small bundles of DNA molecules.

To create the nanoscale stencil masks, we use double-side polished  $\langle 100 \rangle$  silicon wafers with 100 nm of low-stress silicon nitride deposited on each side.<sup>5</sup> Specific regions of the silicon substrate are removed using photolithography and anisotropic etching in an aqueous KOH solution to leave suspended silicon nitride membranes with sizes ranging from 10 to 500  $\mu$ m (Figure 1a). Mask patterns are defined by electron beam lithography using a system based on a JEOL 6400 scanning electron microscope with an Elphy Plus control system (Raith, Inc.). After developing the PMMA electron beam resist, the silicon nitride membrane is etched through using a SF<sub>6</sub> plasma. Etching is done to ensure that the pattern is transferred with high fidelity from the electron beam resist to the silicon nitride membrane. Minimum feature sizes of 50 nm are achieved routinely, although features on

\* Corresponding author. E-mail: cjohnson@dept.physics.upenn.edu.

<sup>†</sup> Current address: Department of Materials Science and Engineering, University of Illinois at Urbana-Champaign, Urbana, Illinois 61801.

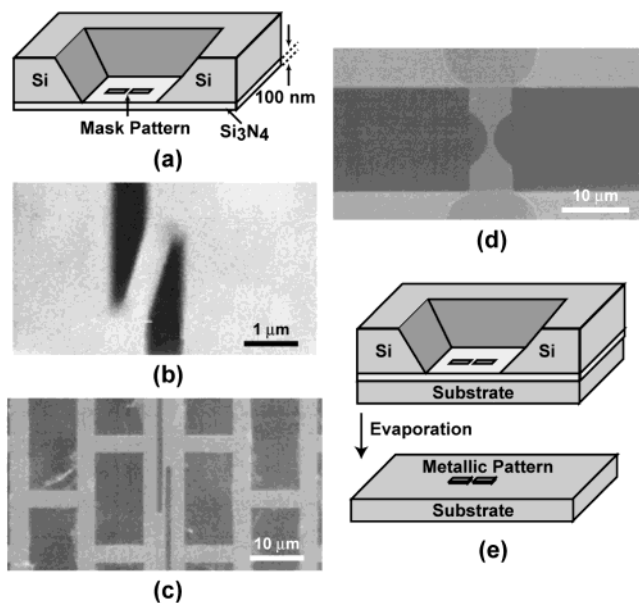


**Figure 1.** (a) Schematic of a nanoscale stencil. (b) SEM image of a mask with electrodes separated by 500 nm over a length of 2  $\mu\text{m}$ . The stencil is distorted by stress in the membrane. (c) SEM image of a mask with electrodes separated by 1  $\mu\text{m}$  over 10  $\mu\text{m}$  in length. The remaining silicon nitride is light gray; holes etched through the membrane are dark gray. The rectangular holes in the membrane relieve the stress and give an undistorted pattern. (d) SEM image of a mask for electrodes separated by a 1- $\mu\text{m}$  gap fabricated from a 20- $\mu\text{m}$ -wide membrane. All silicon nitride in the membrane is removed except the part left for the formation of the gap. (e) Schematic for the fabrication of metallic contacts by shadow mask evaporation.

the scale of 500 nm to 1  $\mu\text{m}$  were used to fabricate the samples described below.

When released from the silicon substrate, the silicon nitride membranes are under considerable tension. Asymmetric stencil patterns can be distorted by stress in the membrane (Figure 1b), leaving the stencil useless. This difficulty is overcome by opening additional stress-relieving holes in the membrane (Figure 1c) or using narrow membranes and symmetric pattern designs (Figure 1d). When the geometry is optimized, stencils are robust and with care can be used up to 15 times as evaporation masks before failure. Electrode fabrication is accomplished by placing the nanoscale stencil in direct contact with a flat substrate (e.g., oxidized silicon or freshly cleaved mica) with predeposited nanowires on the surface and evaporating metal through the stencil (Figure 1e). The choice of contact metallization is flexible: the use of an adhesion layer is optional because there is no “lift-off” processing step. In these experiments, no effort was made to align the stencil with respect to the sample substrate, but this limitation could be overcome in future work. Annealing protocols are sometimes used to improve contacts to nanowires or nanotubes; our process is compatible with this approach, but none of the samples discussed here were treated in this manner.

To fabricate nanotube-based molecular circuits, we first grow SWNTs by catalytic CVD on an oxidized silicon substrate using an iron(III) nitrate solution (50 mg in 1 L of 2-propanol) as the catalyst source following refs 6 and 7.

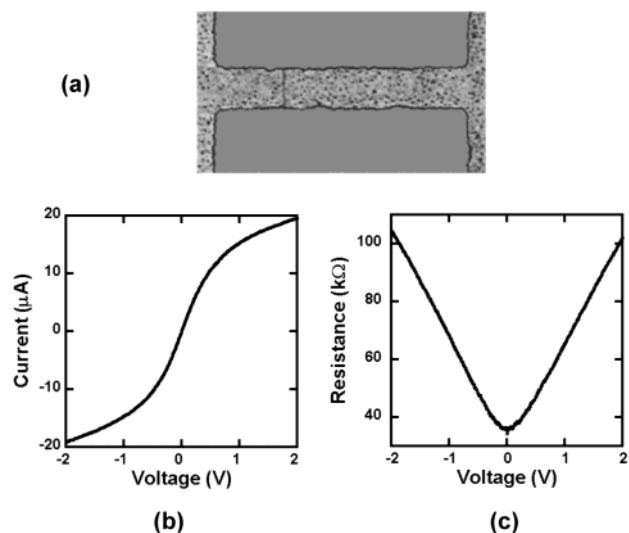


**Figure 2.** (a) AFM image (6  $\mu\text{m} \times 10 \mu\text{m}$ ) of a typical nanotube sample contacted by shadow mask evaporation. (b)  $I$ - $V$  characteristic of a different nanotube sample fabricated by shadow mask evaporation. (c) Resistance ( $V/I$ ) vs voltage for the sample in Figure 2b. The low-bias resistance is 36 k $\Omega$ ; we use the model of ref 8 to extract a saturation current of 28  $\mu\text{A}$ , consistent with transport through a single metallic nanotube.

Atomic force microscopy (AFM) images show nanotube densities of 1 to 20 nanotubes per (20  $\mu\text{m}$ )<sup>2</sup> area. Stencil dimensions are chosen so that on average only one nanotube is contacted by the 15-nm Au contact metallization. Figure 2a is an AFM image of a typical sample, with a nanotube of diameter 1.2 nm contacted by electrodes separated by 1.5  $\mu\text{m}$ . Figure 2b shows the  $I$ - $V$  characteristic of a (different) 1.1-nm diameter metallic nanotube measured under ambient conditions. The low-bias resistance is 36 k $\Omega$ , and current saturation is evident at high voltage bias, with a current density that exceeds 10<sup>9</sup> A/cm<sup>2</sup>. A plot of  $V/I$  versus  $V$  shows linear behavior predicted by Kane’s phonon emission model for current saturation in such devices.<sup>8</sup> More than 20 stencil-contacted samples characterized to date display contact resistances and  $V/I$  versus  $V$  behavior that are similar to what we find for nanotubes contacted using conventional electron beam lithography.<sup>9</sup> Metallic nanotubes contacted using the resist-free stencil, however, seem to be more robust to thermal stress from Joule heating, routinely sustaining 1000- $\mu\text{W}$  input power compared to 200–300  $\mu\text{W}$  for samples contacted by conventional means.<sup>10</sup> Results of further investigations of SWNT samples contacted by this technique will be reported separately.<sup>11</sup>

We now turn to experiments that take full advantage of the chemical-free nature of this contact fabrication scheme. To date, we have focused on circuits consisting of nanofibers of electronic polymers (results reported elsewhere)<sup>12</sup> and networks of  $\lambda$ -DNA. Both of these materials would be destroyed by the solvents used in conventional electron beam lithography; the stencil approach is an excellent way to conduct transport measurements on such samples with submicrometer contact separation. Moreover, our experiments on DNA are among the few to date that combine a contact separation of 1  $\mu\text{m}$  or less with a leads-on-top geometry. In this way, we probe DNA conductivity on small length scales

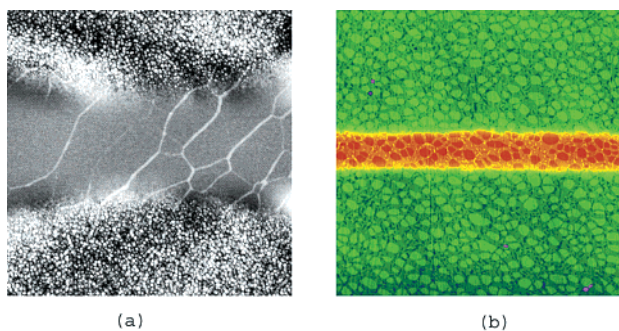


**Figure 3.** (a) AFM height image of several small DNA ropes contacted by gold leads separated by  $1\ \mu\text{m}$ . The height of the DNA ropes is roughly  $1.7\ \text{nm}$ . The scan width is  $2.5\ \mu\text{m}$ . (b) AFM height image of a dense DNA network contacted by  $15\text{-nm}$ -thick,  $12\text{-}\mu\text{m}$ -wide AuPd leads separated by  $1\ \mu\text{m}$ . The height of the network is about  $2\ \text{nm}$ , and the scan size is  $8\ \mu\text{m}$ .

and avoid barriers to electron transport that may form at the kink in the semiflexible molecular wire (e.g., SWNTs<sup>13</sup> or DNA) where it passes over the contact metallization.

To deposit DNA molecules on mica, we use a commercial DNA solution of  $500\ \mu\text{g}/\text{mL}$  duplex  $\lambda$ -DNA in an aqueous solution of  $10\ \text{mM}$  Tris buffer (tris(hydroxymethyl)aminomethane hydrochloride) and  $1\ \text{mM}$  EDTA (ethylenediaminetetraacetic acid) supplied by Biolabs Inc. This is first diluted by a ratio varying from 10 to 100 with a solution of  $11\ \text{mM}$   $\text{MgCl}_2$  and  $10\ \text{mM}$  Tris. Magnesium ions in the solution are used to enhance the attraction of DNA molecules to the mica surface. A  $10\text{-}\mu\text{L}$  droplet of the diluted solution is applied to a freshly cleaved mica substrate. After incubating in air for 2 to 3 min, the sample is rinsed in sterilized water and spun dry. The sample is transferred immediately to the thermal evaporation system, and metallic contacts are deposited through the nanoscale stencil. The evaporation sample stage is water-cooled to avoid damage to the DNA due to heating.

Figure 3a is an AFM topograph of a sparse DNA network deposited using a 100-fold dilution (see above), contacted by electrodes separated by a  $1\text{-}\mu\text{m}$  gap. The height of the threadlike structures in the image is  $1.7\ \text{nm}$ , implying that they are small ropes of a few DNA molecules. For this sample, we designed leads with rounded ends so that conduction would be dominated by just a few strands. All 10 samples fabricated with this geometry had a resistance that exceeded  $1\ \text{T}\Omega$ , the limit of the probe station used to measure them.

To determine more clearly whether DNA has a measurable conductivity and to address the issue of whether larger bundles of DNA might conduct more readily than very small ropes, we made measurements on dense DNA networks prepared using a 10-fold dilution (see above). A typical sample is shown in Figure 3b. The height of the strands in the network is  $2\ \text{nm}$ , so the network consists of flat “rafts” that are one or two DNA molecules in thickness. The contacts for these samples were fabricated from AuPd and designed to be  $12\ \mu\text{m}$  wide, separated by a gap of  $1\ \mu\text{m}$ , so that many DNA molecules contribute in parallel to the conduction. We estimate that thousands of DNA network paths connect the

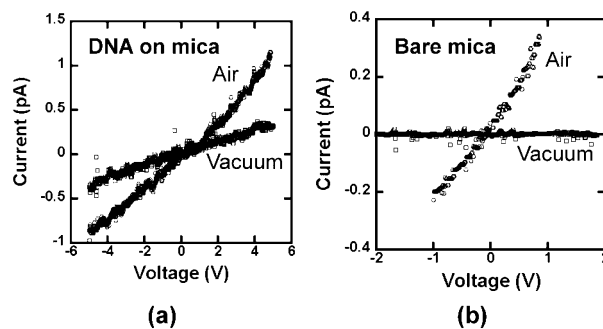


**Figure 4.** (a)  $I$ - $V$  characteristics of a dense DNA network (Figure 3b) in air and vacuum. (b)  $I$ - $V$  characteristics in air and vacuum of a bare mica sample with electrodes identical to those of the circuit in Figure 4a.

electrodes; because  $\lambda$ -DNA strands average  $2\ \mu\text{m}$  in length, we expect hundreds of molecules to span the gap without a break. The AuPd electrodes have very fine and regular grains so that the structure of the DNA strands that lie beneath the contacts can be effectively imaged by AFM. Such images (e.g., Figure 3b) show no signs of damage to the DNA caused by the metal deposition. We made electrical measurements on five samples of this type in air using a probe station; all had an electrical resistance that exceeded  $1\ \text{T}\Omega$ . From these data, we find an upper limit for the conductivity of  $\lambda$ -DNA on mica of  $10^{-5}\ \text{S}/\text{cm}$ , similar to that of an undoped conducting polymer.<sup>14</sup>

We also measured several samples of this type under vacuum ( $10^{-5}$ – $10^{-6}$  Torr) in a system capable of measuring resistances as large as  $50\ \text{T}\Omega$ . Figure 4a shows  $I$ - $V$  characteristics in air and vacuum for the DNA network sample of Figure 3b. In air, we observe a resistance of  $5\ \text{T}\Omega$ ; the resistance increases to  $13\ \text{T}\Omega$  in vacuum. When the sample is returned to air, the conductivity recovers after several hours. For comparison, we measured a sample of bare mica (no DNA deposition) with the same electrode pattern (Figure 4b). The resistance is  $3.5\ \text{T}\Omega$  in air, similar to that of the sample with DNA. Under vacuum, however, the resistance was much larger than that of the DNA sample, exceeding the  $50\text{-T}\Omega$  limit of the measurement setup.

We measured 10 such samples with dense DNA networks. The typical resistance was  $1$ – $5\ \text{T}\Omega$  in air and  $10$ – $20\ \text{T}\Omega$  in vacuum, giving a lower limit of  $1000\ \text{T}\Omega$  for a DNA molecule on mica in vacuum spanning a  $1\text{-}\mu\text{m}$  gap. From these measurements, we conclude that in air, conduction is primarily through a layer of water on the hydrophilic mica surface. In vacuum, this conduction path is eliminated, and we may be able to observe the conductivity of dry DNA on mica. At this point, we cannot rule out the possibility that the low measured conductivity is due to high contact resistance at the DNA–metal contact. Our resistance values in air agree with other reports of low or negligible DNA conductivity.<sup>15–18</sup> We find much lower conductivity for small DNA bundles in vacuum than reported in refs 19 and 20. Our conductivity value is also lower than that reported by Rakitin et al.,<sup>21</sup> perhaps because their bundles were larger diameter and therefore retained more water in their interior under vacuum. This water might facilitate conduction either

directly (i.e., conduction through the water itself) or indirectly through its effects on the structure and flexibility of the DNA and the mobility of its ionic environment.<sup>22</sup> Furthermore, the interaction with the substrate is more important for experiments such as ours, in which most of the DNA is in direct contact with the mica surface. For example, one can imagine that pinning the DNA to the mica surface may cause small distortions that could have an important effect on conductivity.<sup>23</sup>

In conclusion, with nanoscale shadow masks defined in a free-standing silicon nitride membrane, we can contact molecular nanowires without any damage from the chemicals and heat treatment associated with conventional lithography. A high yield of useful devices can be achieved by controlling the density of deposited nanowires and the contact geometry. Measurements on CVD-grown single-walled carbon nanotube samples show properties similar to those of circuits fabricated using conventional techniques, although metallic nanotubes contacted by shadow mask evaporation appear to be significantly more robust under high voltage bias.  $\lambda$ -DNA networks on mica substrates contacted in a leads-on-top geometry showed only very weak conductivity, with an upper bound of  $10^{-5}$  S/cm.

**Acknowledgment.** We thank Scott Paulson for helpful discussions. This work was supported by the Laboratory for Research on the Structure of Matter (NSF DMR00-79909) and the National Science Foundation NIRT (PHY-0103552).

## References

- (1) Ono, K.; Shimada, H.; Kobayashi S.; Ootuka, Y. *Jpn. J. Appl. Phys.* **1996**, *35*, 2369.
- (2) Ullom, J. N.; Fisher, P. A.; Nahum, M. *Phys. Rev. B* **1998**, *58*, 8225.

- (3) Stamm, C.; Marty, F.; Vaterlaus, A.; Weich, V.; Egger, S.; Maier, U.; Ramsperger, U.; Fuhrmann, H.; Pescia, D. *Science* **1998**, *282*, 449.
- (4) Deshmukh, M. M.; Ralph, D. C.; Thomas, M.; Silcox, J. *Appl. Phys. Lett.* **1999**, *75*, 1631.
- (5) Wafers were purchased from the U.C. Berkeley Microfabrication Laboratory ([www-microlab.eecs.berkeley.edu](http://www-microlab.eecs.berkeley.edu)).
- (6) Freitag, M.; Radosavljevic, M.; Zhou, Y. X.; Johnson, A. T. *Appl. Phys. Lett.* **2001**, *79*, 3326.
- (7) Hafner, J. H.; Cheung, C. L.; Oosterkamp, T. H.; Lieber, C. M. *J. Phys. Chem. B* **2001**, *105*, 743.
- (8) Yao, Z.; Kane, C. L.; Dekker, C. *Phys. Rev. Lett.* **2000**, *84*, 2941.
- (9) Radosavljevic, M.; Freitag, M.; Johnson, A. T. Unpublished work.
- (10) Collins, P. G.; Hersam, M.; Arnold, M.; Martel, R.; Avouris, Ph. *Phys. Rev. Lett.* **2001**, *86*, 3128.
- (11) Zhou, Y. X.; Hone, J.; Freitag, M.; Paulson, S.; Smith, W. F.; Johnson, A. T. Unpublished work.
- (12) Zhou, Y. X.; Pinto, N. J.; Freitag, M.; Hone, J.; MacDiarmid, A. G.; Johnson, A. T. Unpublished work.
- (13) Bezryadin, A.; Verschueren, A. R. M.; Tans, S. J.; Dekker, C. *Phys. Rev. Lett.* **1998**, *80*, 4036.
- (14) MacDiarmid, A. G. *Rev. Mod. Phys.* **2001**, *73*, 701.
- (15) Braun, E.; Eichen, Y.; Sivan, U.; Ben-Yoseph, G. *Nature* **1998**, *391*, 775.
- (16) De Pablo, P. J.; Moreno-Herrero, F.; Colchero, J.; Herrero, J. G.; Herrero, P.; Baro, A. M.; Ordejon, P.; Soler, J. M.; Artacho, E. *Phys. Rev. Lett.* **2000**, *85*, 4992.
- (17) Storm, A. J.; van Noort, J.; de Vries, S.; Dekker, C. *Appl. Phys. Lett.* **2001**, *79*, 3881.
- (18) Zhang, Y.; Austin, R. H.; Kraeft, J.; Cox, E. C.; Ong, N. P. *Phys. Rev. Lett.* **2002**, *89*, 198102.
- (19) Fink, H. W.; Schonenberger, C. *Nature* **1999**, *398*, 407.
- (20) Kasumov, A. Y.; Kociak, M.; Gueron, S.; Reulet, B.; Volkov, V. T.; Klinov, D. V.; Bouchiat, H. *Science* **2001**, *291*, 280.
- (21) Ratikin, A.; Aich, P.; Papadopoulos, C.; Kobzar, Yu.; Vedenev, A. S.; Lee, J. S.; Xu, J. M. *Phys. Rev. Lett.* **2001**, *86*, 3670.
- (22) Barnett, R. N.; Cleveland, C. L.; Joy, A.; Landman, U.; Schuster, G. B. *Science* **2001**, *294*, 567.
- (23) Kelley, S. O.; Holmlin, R. E.; Stemp, E. D. A.; Barton, J. K. *J. Am. Chem. Soc.* **1997**, *119*, 99861.

NL034512Y